

Simple and Efficient Separation of Atomically Precise Noble Metal Clusters

Atanu Ghosh,^{†,‡} Jukka Hassinen,^{§,‡} Petri Pulkkinen,[#] Heikki Tenhu,[#] Robin H. A. Ras,^{*,§} and Thalappil Pradeep^{*,†}

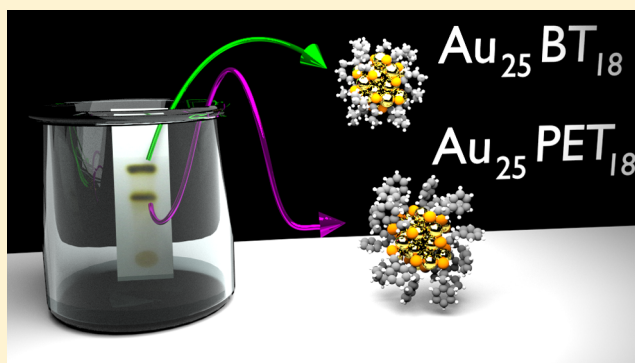
[†]DST Unit of Nanoscience (DST UNS) and Thematic Unit of Excellence (TUE), Department of Chemistry, Indian Institute of Technology Madras, Chennai 600 036, India

[§]Department of Applied Physics, Aalto University (Helsinki University of Technology), Puumiehenkuja 2, FI-02150 Espoo, Finland

[#]Department of Chemistry, University of Helsinki, P.O. Box 55, 00014 Helsinki, Finland

S Supporting Information

ABSTRACT: There is an urgent need for accessible purification and separation strategies of atomically precise metal clusters in order to promote the study of their fundamental properties. Although the separation of mixtures of atomically precise gold clusters $Au_{25}L_{18}$, where L are thiolates, has been demonstrated by advanced separation techniques, we present here the first separation of metal clusters by thin-layer chromatography (TLC), which is simple yet surprisingly efficient. This method was successfully applied to a binary mixture of $Au_{25}L_{18}$ with different ligands, as well as to a binary mixture of different cluster cores, Au_{25} and Au_{144} , protected with the same ligand. Importantly, TLC even enabled the challenging separation of a multicomponent mixture of mixed-monolayer-protected Au_{25} clusters with closely similar chemical ligand compositions. We anticipate that the realization of such simple yet efficient separation technique will progress the detailed investigation of cluster properties.



Atomically precise clusters of noble metals protected with monolayers are some of the most fascinating molecules of contemporary chemical science.^{1–3} Most of the reports on such clusters are concerned with gold, though a few analogues of silver and copper have also appeared in the literature.^{4–10} Molecules such as $Au_{25}SR_{18}$,^{11–13} $Au_{38}SR_{24}$,¹⁴ and $Au_{144}SR_{60}$ ¹⁵ are some of the most stable species in this family of materials. Catalytic and biological applications of such materials are fast evolving.^{2,16–18} Along with this development, we have begun to explore the complex chemistry of these systems.^{19,20} The different chemically nonequivalent environments at their surfaces offer different possibilities for ligand exchange. The possibility of core rearrangement, reduction in size and chirality of the core contribute to the diversity of their chemistry.^{21–23} Whereas some synthesis protocols may produce directly atomically precise metal clusters without the need for separation, other synthesis protocols always yield a mixture of slightly different atomically precise metal clusters and their separation often is a challenge.^{24–26} Efficient methods to isolate the chemically varying species would enhance the growth of science in this area. In this article, we present a simple yet effective way of separating atomically precise clusters, which helps to expand the exploration of their diverse properties.

Although high-pressure liquid chromatography (HPLC),^{27,28} polyacrylamide gel electrophoresis (PAGE),^{24,29} and solvent extraction are used extensively in separating clusters,^{30,31} the

simplest of chromatographic techniques, namely, thin-layer chromatography (TLC) has not been attempted for the separation of such clusters. In the following, we show that differently functionalized clusters of the same core, varying cores with the same chemical functionality and even mixed-monolayer-protected clusters of the same core having only slight structural differences are well separable by a simple TLC methodology. Even though TLC has been used in organic chemistry for a long time, the realization of its applicability to metal clusters adds a new tool in the toolbox of cluster science and further emphasizes the analogous nature of metal clusters and small organic molecules.

EXPERIMENTAL SECTION

Chemicals and Materials. Gold(III) chloride trihydrate ($\geq 99.9\%$), butanethiol (99%), hexanethiol (99%), phenylethanethiol ($\geq 99\%$), sodium borohydride (95%), tetraoctylammonium bromide (TOABr, 98%), and trans-2-[3-(4-*tert*-butylphenyl)-2-methyl-2-propenyldiene]malononitrile (DCTB, $> 98\%$) were purchased from Sigma-Aldrich. Tetrathiolated calix[4]arene (25,26,27,28-tetrakis(4-mercapto-*n*-butoxy)calix-

Received: August 22, 2014

Accepted: November 14, 2014

Published: November 14, 2014

[4]arene) was synthesized according to a reported method.³² All the chemicals were used as received without further purification. All solvents (dichloromethane (DCM), *n*-hexane, tetrahydrofuran (THF) and methanol) were purchased from Sigma or Rankem and were of analytical grade. Silica gel 60 F₂₅₄ TLC plates were purchased from Merck. The water used in syntheses was Milli-Q grade with a resistivity of 18.2 MΩ·cm.

Synthesis of Au₂₅L₁₈ and Mixed Monolayer Au₂₅Calix₀₋₃BT₆₋₁₈ Clusters. Au₂₅BT₁₈ (BT- butanethiolate, C₄H₉S-) and the calixarene-functionalized Au₂₅ clusters were synthesized by a reported method.³² Briefly, HAuCl₄·3H₂O (80 mg) was dissolved in 15 mL of THF and 130 mg of TOABr was added to this vigorously stirred solution. The stirring was continued for 15 min after which the solution was orange-red in color. To this solution, 110 μL of butanethiol in 500 μL of THF (in case of Au₂₅BT₁₈) or a mixture of 110 μL of butanethiol and 4.4 mg of calixarene tetrathiol in 500 μL of THF (in case of Au₂₅Calix₀₋₃BT₆₋₁₈) was rapidly added under vigorous stirring (1200 rpm). The stirring was continued for 2 h during which the solution turned colorless. After that, 78 mg of NaBH₄ dissolved in 5 mL of ice-cold H₂O was rapidly added to the reaction solution under vigorous stirring, and the stirring was continued for 5 h in the case of Au₂₅BT₁₈ and 15 h in the case of Au₂₅Calix₀₋₃BT₆₋₁₈. The solvent was removed from the reaction mixture by rotary vacuum evaporation, and clusters were purified by centrifugal washing with methanol (4 times, 3000 RCF). In the case of Au₂₅BT₁₈, methanol/water mixture (3:1 v/v) was used in centrifugal washing. Subsequently, the product was dissolved to THF, and the white insoluble matter consisting most likely of Au(I)-thiolates was removed by centrifugation. In case of Au₂₅Calix₀₋₃BT₆₋₁₈, the clusters in THF were further purified by size-exclusion chromatography (stationary phase Bio-Rad Bio-Beads S-X1 200–400 Mesh) to remove a small amount of larger clusters. Au₂₅PET₁₈ (PET-phenylethanethiolate, PhCH₂CH₂S-) and Au₂₅HT₁₈ (HT-hexanethiolate, C₆H₁₃S-) were synthesized following the same procedure, and 136 and 144 μL thiol were added for the synthesis of Au₂₅PET₁₈ and Au₂₅HT₁₈, respectively.

Synthesis of Au₂₅PET₁₈ and Au₁₄₄PET₆₀ Mixture. A crude mixture of Au₂₅PET₁₈ and Au₁₄₄PET₆₀ was synthesized in a single batch according to a reported method.³⁰ HAuCl₄·3H₂O (120 mg) was dissolved in 15 mL of methanol, and 193 mg of TOABr was added to this vigorously stirred solution. The stirring was continued for 15 min after which the solution was orange-red in color. To this solution, 216 μL of phenylethanethiol was added, and the mixture was stirred for 15 min. After that, 115 mg of NaBH₄ dissolved in 6 mL of ice-cold H₂O was rapidly added to the reaction mixture. The stirring was continued for 5 h at room temperature, after which the precipitated clusters were collected by centrifugation and washed with methanol 5 times. The crude product containing Au₂₅PET₁₈ and Au₁₄₄PET₆₀ was dissolved in DCM and precipitate consisting of insoluble Au-thiolates was removed. DCM solution was rotary evaporated to dryness and spotted on the TLC plate for separation.

TLC Separation. The cluster samples (1 μL) were pipetted to TLC plates and dried in air. After drying, the plate was eluted with DCM/hexane mixture (the optimal solvent ratio varies with cluster system). After the separation, the bands were cut from the TLC plate, and the clusters from each band were individually extracted with DCM. The solids (pieces of TLC plate) were removed from these extracts by centrifugation. The

retention factors (*R_f*) for all separated clusters are given in the Supporting Information (Table S-1).

Characterization. Absorption spectra of clusters were recorded in UV–vis range with PerkinElmer Lambda 25 UV–vis absorption spectrophotometer. Clusters were dissolved to DCM and spectra recorded in quartz cells with 10 mm path length. Matrix-assisted laser desorption ionization (MALDI) mass spectra of clusters were collected using either of two different linear time-of-flight mass spectrometers: Voyager DE PRO (Applied Biosystems) or Autoflex II (Bruker Daltoniks). Both mass spectrometers were equipped with UV N₂ lasers (337 nm) and provided similar results. DCTB in DCM (12.5 mg/mL) was used as the matrix. The measurements were performed in positive ion mode. For each measurement, typically 500 scans were acquired.

RESULTS AND DISCUSSION

Separation of Binary Mixture of Au₂₅L₁₈, L = BT/HT/PET. In Figure 1, we show the separation of Au₂₅HT₁₈ (HT-hexanethiolate, C₆H₁₃S-) and Au₂₅BT₁₈ (BT- butanethiolate, C₄H₉S-) from a mixture of two, even though the polarity difference of BT and HT is very small. A mixture of clusters was spotted on the TLC plate and then eluted using DCM/hexane mixture. For this system, the best separation occurred at a DCM/hexane ratio of 40:60 (unless otherwise noted, the solvent ratios are expressed as volume ratios throughout the manuscript). A photograph of the two separated bands is shown in Figure 1A. After optimization of the solvent mixture, preparative scale separation was performed by simultaneously eluting multiple spots of this mixture. The separated bands 1 and 2 were cut off from the plate and individually extracted using DCM. The UV–vis spectra of band 1 (red) and band 2 (blue) show characteristic absorption features originating from the Au₂₅ core (Figure 1).

To verify the identity of these bands, we performed MALDI MS using DCTB as the matrix which is known to enhance intact ionization for this system at threshold laser powers.³³ MALDI MS data of bands 1 (red) and 2 (blue) are shown in

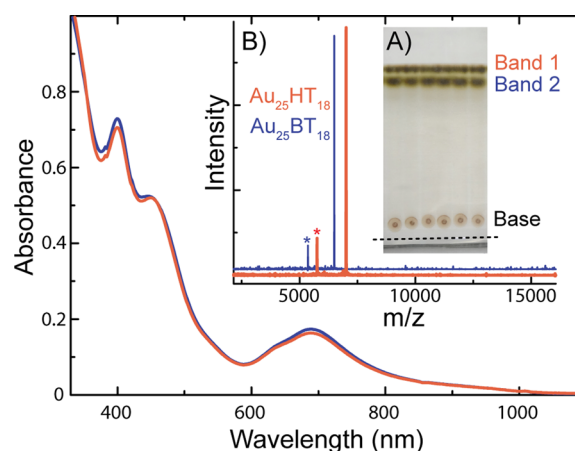


Figure 1. UV–vis spectra of the TLC separated materials. (A) Photograph of the TLC plate used for cluster separation. Bands 1 and 2 are due to two separated clusters. The base shows the location where the mixture was spotted. The level of liquid is marked with a dashed line. (B) MALDI MS data of TLC separated materials confirming that bands 1 (red trace) and 2 (blue trace) are pure Au₂₅HT₁₈ and Au₂₅BT₁₈, respectively. The fragmented product, Au₂₁L₁₄ is shown with an asterisk (*) in each trace.

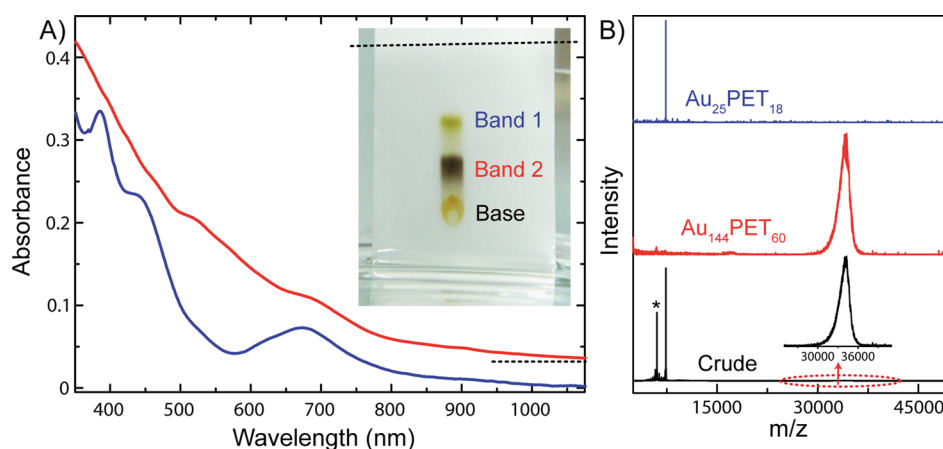


Figure 2. (A) UV-vis spectra of the two bands separated by TLC. Red trace matches well with the previously reported UV-vis spectrum of $\text{Au}_{144}\text{PET}_{60}$ cluster,¹⁵ and blue trace matches with the UV-vis spectrum of $\text{Au}_{25}\text{PET}_{18}$ cluster.¹¹ The red trace has been vertically shifted for clarity. Inset: photograph of the TLC plate used for cluster separation (solvent front marked as a dashed line). (B) MALDI MS data of crude (black trace) and isolated clusters (blue and red trace) confirming that bands 1 and 2 consist of isolated $\text{Au}_{25}\text{PET}_{18}$ and $\text{Au}_{144}\text{PET}_{60}$, respectively. The fragmented product, $\text{Au}_{21}\text{L}_{14}$, is shown with an asterisk (*).

Figure 1B, thus confirming that bands 1 and 2 correspond to $\text{Au}_{25}\text{HT}_{18}$ and $\text{Au}_{25}\text{BT}_{18}$, respectively. We have also separated BT and PET protected Au_{25} using the same methodology. Both the clusters were spotted on the same spot of the TLC plate and then eluted immediately using DCM/hexane mixture. For this system, the best separation occurs at a DCM/hexane ratio of 60:40. Details about this separation are given in Supporting Information (Figure S-1). Figure S-1A shows the photograph of two separated bands on the TLC plate. MALDI MS data (S-1B) confirms that bands 1 (black) and 2 (red) correspond to $\text{Au}_{25}\text{BT}_{18}$ and $\text{Au}_{25}\text{PET}_{18}$, respectively.

Analogously to TLC separation of small organic molecules, the choice of solvent polarity plays a key role in deciding the extent of separation of clusters. In 100% DCM, all the Au_{25} clusters elute along with the solvent front, and thus, no separation occurred in either BT-HT or BT-PET system. In both systems, a slight decrease of solvent polarity reduces the movement of clusters on the TLC plate, resulting in a clear separation of the two bands. For the BT-HT system, we have decreased the polarity of the solvent mixture more than that used in the BT-PET system. In the former case, the movement of clusters on the TLC plate should be slow to get a better separation as the polarity difference between BT and HT is very small in comparison to BT-PET system.

It is worth noting that, based on the UV-vis spectra in Figure 1, the charge of the separated clusters is neutral. $\text{Au}_{25}\text{L}_{18}$ clusters have two significantly stable oxidation states, namely, $\text{Au}_{25}\text{L}_{18}^{-}$ and $\text{Au}_{25}\text{L}_{18}^0$, which can be converted from one to another by electrochemistry³⁴ and by exposure to oxidizing or reducing agents.³⁵ Fresh $\text{Au}_{25}\text{L}_{18}$ synthesis products are typically negative charged. However, these clusters easily oxidize to $\text{Au}_{25}\text{L}_{18}^0$ due to exposure to air and ambient light.^{36,37} When separating freshly prepared $\text{Au}_{25}\text{PET}_{18}$ by TLC, we observed a rapid oxidation during drying and elution of the clusters on the TLC plate (Figure S-2). If drying and elution times are decreased, thus leading to only partial oxidation, even separation of $\text{Au}_{25}\text{L}_{18}^{-}$ and $\text{Au}_{25}\text{L}_{18}^0$ can be realized with TLC, since $\text{Au}_{25}\text{L}_{18}^{-}$ elutes slower than $\text{Au}_{25}\text{L}_{18}^0$ likely due to the attached TOA^+ (Figure S-3).

Separation of Different Cluster Nuclearities. We have also separated a mixture of two different cluster cores, Au_{25} and Au_{144} , protected by the same ligand, PET. The mixture of

clusters was dissolved in a minimum amount of DCM and spotted on a TLC plate. The sample was eluted with a DCM/hexane mixture (60:40), and two separate bands were observed (Figure 2A, inset). The UV-vis spectra of those two isolated bands were measured after extracting them in DCM (Figure 2A). Blue and red traces correspond to bands 1 and 2, respectively, and these traces match with those of $\text{Au}_{25}\text{PET}_{18}$ and $\text{Au}_{144}\text{PET}_{60}$.^{11,15} To confirm the purity of each band, we performed MALDI MS measurements of the crude and isolated bands using DCTB as the matrix. The mass spectrum of the crude product contains both $\text{Au}_{25}\text{PET}_{18}$ and $\text{Au}_{144}\text{PET}_{60}$ (Figure 2B). As ionization efficiency of Au_{25} is considerably higher than that of the bigger cluster Au_{144} , the intensity of MALDI MS peak for the former is higher. Expanded spectrum shows the presence of Au_{144} . Blue and red traces confirm that bands 1 and 2 contain pure Au_{25} and Au_{144} , respectively. Due to its reduced size, Au_{25} elutes faster on the TLC plate. As differently sized clusters can be separated by TLC, we foresee this method to be applicable in monitoring cluster synthesis (see further discussion below).

Separation of Mixed-Monolayer-Protected Clusters.

To further explore the potential of TLC separation, we continued our study with mixed-monolayer-protected Au_{25} clusters, in which the monolayer consisted of BT and tetrathiolate of 25,26,27,28-tetrakis (4-mercapto-*n*-butoxy)calix-[4]arene (Calix, Figure 3 inset). MALDI MS measurements confirmed that the clusters contained 0–3 Calix moieties (Figure 3), which is in agreement with our earlier electrospray ionization mass spectrometric study.³² The MALDI MS data shows that the crude product is composed of several different clusters varying slightly in their monolayer composition ($\text{Au}_{25}\text{Calix}_{0-3}\text{BT}_{6-18}$).

Notably, the tetrathiolated Calix ligands are bound to Au_{25} surface predominantly in tetradentate or bidentate manner leading to the absence of odd numbers of BT ligands on the clusters. Peak positions and molecular compositions are discussed in Supporting Information (Tables S-2 and S-3). This cluster mixture was subjected to TLC with DCM/hexane mixture as the eluent. For this system, the optimal DCM/hexane ratio was found to be 30:70. Even though the clusters elute more slowly in such low polarity media, we observed undesired smearing of bands with higher DCM content. In

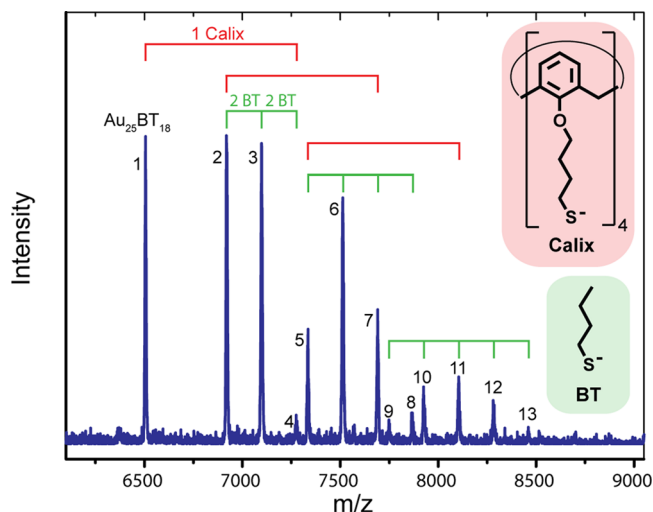


Figure 3. MALDI MS data of $\text{Au}_{25}\text{Calix}_{0-3}\text{BT}_{6-18}$ cluster mixture. Peak spacings of 773 m/z (1 Calix) and 178.4 m/z (2 BT) have been marked for clarity. The compositions of the labeled peaks (1–13) are interpreted in Table S-2. Insets show the structures of the ligands in the mixed-monolayer-protected Au_{25} clusters.

order to achieve a greater separation between the bands, the same TLC plate was eluted several times. Four distinct bands could be separated in this manner, in addition to the immobile base band (Figure 4A). To confirm the identity of these bands, they were extracted and analyzed by MALDI MS using DCTB as the matrix (Figure 4B).

From the MALDI MS data of bands 1–5, it is evident that the fastest eluting clusters are $\text{Au}_{25}\text{BT}_{18}$ (band 1, blue), followed by $\text{Au}_{25}\text{Calix}_1\text{BT}_{16}$ (band 2, green) and $\text{Au}_{25}\text{Calix}_1\text{BT}_{14}$ (band 3, magenta). Surprisingly, even clusters having such minor differences in composition could be separated by TLC. $\text{Au}_{25}\text{Calix}_1\text{BT}_{16}$ is less polar than $\text{Au}_{25}\text{Calix}_1\text{BT}_{14}$ based on the difference in conformation and binding of Calix on the cluster surface, and therefore, it elutes faster (see further discussion below). Furthermore, band 4 is composed of clusters having exclusively two Calix moieties ($\text{Au}_{25}\text{Calix}_2\text{BT}_{10-16}$), whereas the majority of clusters in the immobile base band 5 have three Calix units attached. It is

worthwhile to mention that no separation of $\text{Au}_{25}\text{Calix}_{0-3}\text{BT}_{6-18}$ clusters could be achieved by size-exclusion chromatography.

Bands 4 and 5 from the TLC run still contain multiple mixed-monolayer compositions. These bands were extracted, combined, and subjected to another TLC run with a slightly higher polarity eluent (DCM/hexane 35:65). Three bands could be extracted from the second run, containing two bands composed of $\text{Au}_{25}\text{Calix}_2\text{BT}_n$ clusters (band 1: $n = 12-14$, band 2: $n = 10-12$) and one band composed of various $\text{Au}_{25}\text{Calix}_{2-4}\text{BT}_{6-12}$ clusters (Figure 5). Thus,

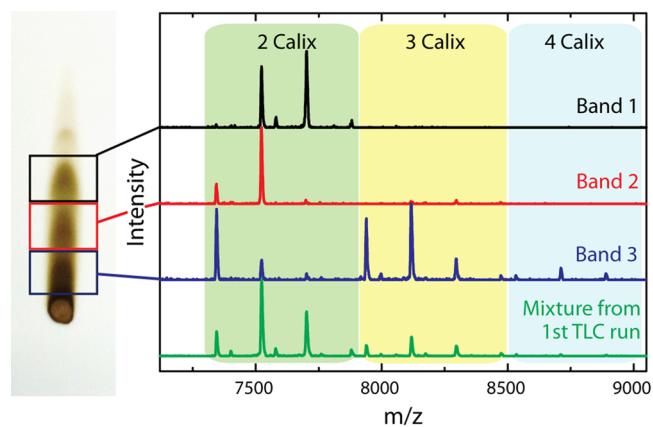


Figure 5. Further TLC separation of $\text{Au}_{25}\text{Calix}_{0-3}\text{BT}_{6-18}$ clusters. Bands 4 and 5 from first TLC run (DCM/hexane 30:70) were combined and subjected to another run with DCM/hexane 35:65 (photograph on the left). Three bands could be extracted and subjected to MALDI MS analysis (right).

$\text{Au}_{25}\text{Calix}_2\text{BT}_{10-16}$ clusters could be separated into two fractions (bands 1 and 2), which were not separable in the first TLC run because they were retained near the base band. Thus, it is possible to separate more products by running the TLC of third band again by tuning the polarity of the eluent. It is also noteworthy that separation can reveal new cluster compositions. Note that clusters having four Calix moieties were not observed in MALDI MS of the crude

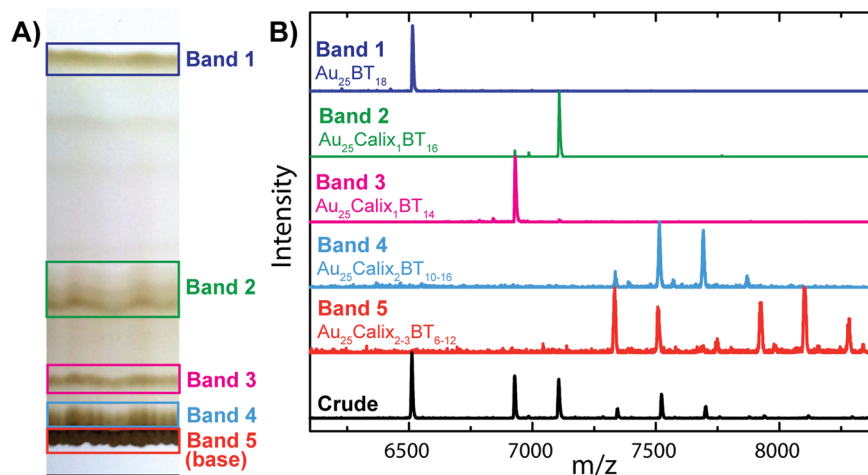


Figure 4. (A) Photograph of the TLC plate used for cluster separation. The faint bands observed between bands 1 and 2 are caused by sticking of the clusters to the TLC plate upon drying between runs. (Note that the TLC plates were eluted repeatedly. See also Supporting Information, Figure S-4.) (B) MALDI MS data of $\text{Au}_{25}\text{Calix}_{0-3}\text{BT}_{6-18}$ crude product before TLC (black trace) and bands 1–5 separated by TLC.

$\text{Au}_{25}\text{Calix}_{0-3}\text{BT}_{6-18}$ product because of suppression due to more abundant species (Figure 3).

On the basis of the TLC data, we can also derive qualitative information about the polarity of clusters. As seen from the clusters containing only one Calix unit, those having more BT ligands are less polar. Based on the results from the second TLC separation, this rule seems to hold also for clusters with two and three Calix moieties. Clusters having more BT ligands have more Calix ligands bound with two thiolates. On the other hand, clusters with a smaller amount of BT have more Calix ligands bound with four thiolates. These two binding modes explain the polarity differences of the clusters: Binding with four thiolates exposes the polar ether groups of Calix, whereas two thiolate binding causes pinching of the calixarene cone, thus shielding the polar oxygen atoms.

Purification of Clusters from Excess Thiol and Monitoring Cluster Synthesis. Excess thiol is a common impurity in thiolate-protected cluster samples despite rigorous washing of clusters after synthesis. In Figure 6, we show that

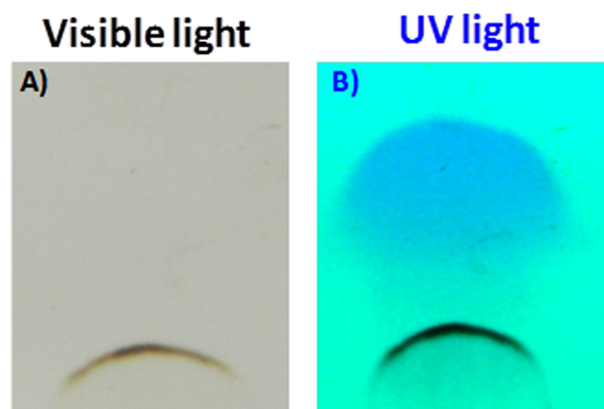


Figure 6. Photographs of TLC separation of small amount of thiol present in methanol-washed $\text{Au}_{25}\text{PET}_{18}$. (A) and (B) are the photographs of same TLC plate under visible and UV light, respectively.

TLC method can be used to remove this small amount of excess thiol typically present after the synthesis. Initially, the sample was eluted with DCM/hexane mixture (70:30) to get a band. Then the sample was further eluted with 100% hexane three times. The TLC of a four-times-methanol-washed $\text{Au}_{25}\text{PET}_{18}$ cluster revealed a fast moving colorless band due to excess phenylethanethiol, which is visible under UV light (Figure 6).

We have also shown that it is possible to monitor the progress of cluster synthesis by TLC. In Supporting Information (Figure S-5), we have presented the time-dependent TLC of synthesis of $\text{Au}_{25}\text{PET}_{18}$. In this experiment, aliquots of the raw cluster mixture were precipitated by addition of water and further washed with methanol to quickly remove most of the excess thiol. Thereafter, the clusters were spotted to a TLC plate and eluted with hexane to completely remove the remaining thiol. Subsequently, the clusters were eluted with DCM/hexane 60:40.

Initially, a mixture of clusters is formed as shown in Figure S-5A after 1 and 3 h of reaction. The fraction of larger clusters decreases as the reaction proceeds and after 8 h, and TLC of the sample shows a single band (Figure S-5A, right). It implies that the synthesis of $\text{Au}_{25}\text{PET}_{18}$ was completed after 8 h. The bands after 1 h of reaction were individually extracted with

DCM and further purified by another TLC run. The bands were analyzed by MALDI MS (Figure S-5B). These data show that the top band (band 1) consists of $\text{Au}_{25}\text{PET}_{18}$ clusters, as expected. Slightly below the $\text{Au}_{25}\text{PET}_{18}$ band, we observed a band mainly composed of $\text{Au}_{38}\text{PET}_{24}$ and $\text{Au}_{40}\text{PET}_{24}$ clusters. Moreover, bands 3 and 4 were found to contain multiple larger clusters in the size range of 12 000–15 000 m/z and 14 000–21 000 m/z , respectively. In addition, band 3 produced a strong MALDI MS signal of $\text{Au}_{67}\text{PET}_{35}$ cluster.³⁸ This experiment further validates that clusters of different nuclearities can be separated by TLC. We foresee TLC as a highly applicable tool in monitoring cluster synthesis that advances the understanding of reaction pathways leading to specific clusters and provides a straightforward way for optimization of synthetic methods.

CONCLUSIONS

In summary, we have shown the surprisingly efficient TLC separation of atomically precise clusters of gold varying in ligand structure, core size, and mixed-monolayer composition. The data presented show that simple, inexpensive chromatographic tools can be used for the isolation of monolayer-protected clusters, although they are chemically complex. We anticipate that such a simple, broadly applicable methodology will enhance the detailed investigation and understanding of chemical and photophysical properties of well-defined cluster systems.

ASSOCIATED CONTENT

Supporting Information

Additional information as noted in text. This material is available free of charge via the Internet at <http://pubs.acs.org>.

AUTHOR INFORMATION

Corresponding Authors

*E-mail: pradeep@iitm.ac.in. Fax: +91-44-2257-0509/0545.

*E-mail: robin.ras@aalto.fi. Fax: +358-9-47023155.

Author Contributions

[‡]A.G. and J.H. contributed equally.

Notes

The authors declare no competing financial interest.

ACKNOWLEDGMENTS

The authors thank the Department of Science and Technology, Government of India (DST) and the Academy of Finland for funding through an Indo-Finland initiative. Equipment support was provided by the Nano Mission of the Government of India. A.G. thanks the CSIR for a research fellowship. This work was supported by the Academy of Finland through its Centres of Excellence Programme (2014–2019).

REFERENCES

- (1) Mathew, A.; Pradeep, T. *Part. Part. Syst. Charact.* **2014**, *31*, 1017–1053.
- (2) Qian, H.; Zhu, M.; Wu, Z.; Jin, R. *Acc. Chem. Res.* **2012**, *45*, 1470–1479.
- (3) Häkkinen, H. *Nat. Chem.* **2012**, *4*, 443–455.
- (4) Yang, H.; Wang, Y.; Huang, H.; Gell, L.; Lehtovaara, L.; Malola, S.; Häkkinen, H.; Zheng, N. *Nat. Commun.* **2013**, *4*, 2422.
- (5) Desireddy, A.; Conn, B. E.; Guo, J.; Yoon, B.; Barnett, R. N.; Monahan, B. M.; Kirschbaum, K.; Griffith, W. P.; Whetten, R. L.; Landman, U.; Bigioni, T. P. *Nature* **2013**, *501*, 399–402.

- (6) Chakraborty, I.; Govindarajan, A.; Erusappan, J.; Ghosh, A.; Pradeep, T.; Yoon, B.; Whetten, R. L.; Landman, U. *Nano Lett.* **2012**, *12*, 5861–5866.
- (7) Rao, T. U. B.; Nataraju, B.; Pradeep, T. *J. Am. Chem. Soc.* **2010**, *132*, 16304–16307.
- (8) Negishi, Y.; Arai, R.; Niihori, Y.; Tsukuda, T. *Chem. Commun.* **2011**, *47*, 5693–5695.
- (9) Nishida, N.; Yao, H.; Kimura, K. *Langmuir* **2008**, *24*, 2759–2766.
- (10) Ganguly, A.; Chakraborty, I.; Udayabhaskararao, T.; Pradeep, T. *J. Nanopart. Res.* **2013**, *15*, 1522/1.
- (11) Shichibu, Y.; Negishi, Y.; Tsukuda, T.; Teranishi, T. *J. Am. Chem. Soc.* **2005**, *127*, 13464–13465.
- (12) Zhu, M.; Aikens, C. M.; Hollander, F. J.; Schatz, G. C.; Jin, R. *J. Am. Chem. Soc.* **2008**, *130*, 5883–5885.
- (13) Heaven, M. W.; Dass, A.; White, P. S.; Holt, K. M.; Murray, R. W. *J. Am. Chem. Soc.* **2008**, *130*, 3754–3755.
- (14) Qian, H.; Eckenhoff, W. T.; Zhu, Y.; Pintauer, T.; Jin, R. *J. Am. Chem. Soc.* **2010**, *132*, 8280–8281.
- (15) Qian, H.; Jin, R. *Nano Lett.* **2009**, *9*, 4083–4087.
- (16) Zhu, Y.; Qian, H.; Drake, B. A.; Jin, R. *Angew. Chem., Int. Ed.* **2010**, *49*, 1295–1298.
- (17) Habeeb Muhammed, M. A.; Verma, P. K.; Pal, S. K.; Retnakumari, A.; Koyakutty, M.; Nair, S.; Pradeep, T. *Chem.—Eur. J.* **2010**, *16*, 10103–10112.
- (18) de Silva, N.; Ha, J.-M.; Solovyov, A.; Nigra, M. M.; Ogino, I.; Yeh, S. W.; Durkin, K. A.; Katz, A. *Nat. Chem.* **2010**, *2*, 1062–1068.
- (19) Mathew, A.; Natarajan, G.; Lehtovaara, L.; Häkkinen, H.; Kumar, R. M.; Subramanian, V.; Jaleel, A.; Pradeep, T. *ACS Nano* **2014**, *8*, 139–152.
- (20) Ghosh, A.; Pradeep, T.; Chakrabarti, J. *J. Phys. Chem. C* **2014**, *118*, 13959–13964.
- (21) Nimmala, P. R.; Jupally, V. R.; Dass, A. *Langmuir* **2014**, *30*, 2490–2497.
- (22) Knoppe, S.; Bürgi, T. *Acc. Chem. Res.* **2014**, *47*, 1318–1326.
- (23) Zeng, C.; Liu, C.; Pei, Y.; Jin, R. *ACS Nano* **2013**, *7*, 6138–6145.
- (24) Negishi, Y.; Nobusada, K.; Tsukuda, T. *J. Am. Chem. Soc.* **2005**, *127*, 5261–5270.
- (25) Udaya Bhaskara Rao, T.; Pradeep, T. *Angew. Chem., Int. Ed.* **2010**, *49*, 3925–3929.
- (26) Negishi, Y.; Sakamoto, C.; Ohyama, T.; Tsukuda, T. *J. Phys. Chem. Lett.* **2012**, *3*, 1624–1628.
- (27) Niihori, Y.; Matsuzaki, M.; Pradeep, T.; Negishi, Y. *J. Am. Chem. Soc.* **2013**, *135*, 4946–4949.
- (28) Dolamic, I.; Knoppe, S.; Dass, A.; Bürgi, T. *Nat. Commun.* **2012**, *3*, 1802/1.
- (29) Kimura, K.; Sugimoto, N.; Sato, S.; Yao, H.; Negishi, Y.; Tsukuda, T. *J. Phys. Chem. C* **2009**, *113*, 14076–14082.
- (30) Qian, H.; Jin, R. *Chem. Mater.* **2011**, *23*, 2209–2217.
- (31) Knoppe, S.; Boudon, J.; Dolamic, I.; Dass, A.; Bürgi, T. *Anal. Chem.* **2011**, *83*, 5056–5061.
- (32) Hassinen, J.; Pulkkinen, P.; Kalenius, E.; Pradeep, T.; Tenhu, H.; Häkkinen, H.; Ras, R. H. A. *J. Phys. Chem. Lett.* **2014**, *5*, 585–589.
- (33) Dass, A.; Stevenson, A.; Dubay, G. R.; Tracy, J. B.; Murray, R. W. *J. Am. Chem. Soc.* **2008**, *130*, 5940–5946.
- (34) Tofanelli, M. A.; Ackerson, C. J. *J. Am. Chem. Soc.* **2012**, *134*, 16937–16940.
- (35) Zhu, M.; Aikens, C. N.; Hendrich, M. P.; Gupta, R.; Qian, H.; Schatz, G. C.; Jin, R. *J. Am. Chem. Soc.* **2009**, *131*, 2490–2492.
- (36) Zhu, M.; Eckenhoff, W. T.; Tomislav, P.; Jin, R. *J. Phys. Chem. C* **2008**, *112*, 14221–14224.
- (37) Kauffman, D. R.; Alfonso, D.; Matranga, C.; Li, G.; Jin, R. *J. Phys. Chem. Lett.* **2013**, *4*, 195–202.
- (38) Nimmala, P. R.; Yoon, B.; Whetten, R. L.; Landman, U.; Dass, A. *J. Phys. Chem. A* **2013**, *117*, 504–517.